J. Korean Soc. Ind. Appl. Math. Vol.27, No.4, 245–271, 2023 https://doi.org/10.12941/jksiam.2023.27.245

SUPERCONVERGENCE AND POSTPROCESSING OF EQUILIBRATED FLUXES FOR QUADRATIC FINITE ELEMENTS

KWANG-YEON KIM[1]

[1]DEPARTMENT OF MATHEMATICS, KANGWON NATIONAL UNIVERSITY, SOUTH KOREA
Email address: eulerkim@kangwon.ac.kr

ABSTRACT. In this paper we discuss some recovery of $H(\mathrm{div})$-conforming flux approximations from the equilibrated fluxes of Ainsworth and Oden for quadratic finite element methods of second-order elliptic problems. Combined with the hypercircle method of Prager and Synge, these flux approximations lead to a posteriori error estimators which provide guaranteed upper bounds on the numerical error. Furthermore, we prove some superconvergence results for the flux approximations and asymptotic exactness for the error estimator under proper conditions on the triangulation and the exact solution. The results extend those of the previous paper for linear finite element methods.

1. INTRODUCTION

A posteriori error estimators play a vital role in efficient implementation of finite element methods through automatic adaptive mesh refinement. The quality of an error estimator η is typically evaluated in terms of the so-called effectivity index $\eta/|||e|||$, where $|||e|||$ denotes the numerical error measured in some norm (e.g., the energy norm) related to the underlying problem. For example, the reliability and efficiency of η are verified by showing that its effectivity index is uniformly bounded above and below by positive constants independent of the mesh size. In early days the error estimators using strong residuals of the discrete solutions were widely studied, but they tend to exhibit rather large effectivity indices. Moreover, their reliability and efficiency results contain positive constants which are generally impossible to trace out.

In the meantime, there has been a great deal of effort in developing other types of a posteriori error estimators which show better performance than traditional residual-based ones. In particular, it is now well known that recovery-based error estimators such as SPR and PPR [5, 6, 7, 8, 9] and Bank–Weiser error estimators [1, 2, 3, 4] very often produce amazingly accurate results in the sense that $\eta/|||e||| \to 1$ as the mesh size tends to zero. This so-called *asymptotic exactness*, however, depends heavily on the structure of the triangulation and the

Received October 30 2023; Revised December 19 2023; Accepted in revised form December 25 2023; Published online December 25 2023.

2020 *Mathematics Subject Classification.* 65N30,65N15.

Key words and phrases. A posteriori error estimation, hypercircle method, asymptotic exactness, superconvergence.

regularity of the exact solution, and is usually established by using the superconvergence property of the discrete solutions.

On the other hand, the hypercircle method of Prager and Synge [10] has the advantage of providing *guaranteed upper bound* $\eta \geq |\!|\!| e |\!|\!|$ under minimal conditions (see, for example, [11, 12, 13, 14, 15, 16, 17, 18, 19, 20, 21]), which can be used in constructing stopping criteria for iterative solvers [22, 23]. This method requires recovery of $H(\mathrm{div})$-conforming flux approximations for primal finite element methods of second-order elliptic problems considered in this paper. For example, one may use the equilibrated fluxes on interelement boundaries [24, Chapter 6] or solve carefully designed local Neumann problems [12, 14, 17] to recover the flux approximations in the Raviart–Thomas spaces. It is worthwhile to mention that the latter recovery techniques offer polynomial-degree-robust efficiency results in contrast to other error estimators.

In the previous paper [25] for *linear* finite elements, we recovered the flux approximation in the lowest order Raviart–Thomas space using the equilibrated fluxes of Ainsworth and Oden, and proved its superconvergence under proper conditions on the triangulation and the exact solution. Moreover, a postprocessing scheme was proposed to improve this flux approximation by adding the curl of a quadratic bump function which minimizes the L^2 error of the flux approximation. This minimization involves solving a global matrix system, but it is very inexpensive due to well-conditioning of the matrix system. This leads to an a posteriori error estimator which achieves not only guaranteed upper bound (in all cases) but also asymptotic exactness when the improved flux approximation is superconvergent.

The purpose of this paper is to extend the results of [25] to *quadratic* finite elements. In the computational aspect, the overall framework is similar to linear finite elements. We first recover a flux approximation in the next-to-lowest order Raviart–Thomas space using the equilibrated fluxes of Ainsworth and Oden, and then improve it by adding the curl of some optimal cubic bump function. On the contrary, in the theoretical aspect, the proof of superconvergence of the flux approximation in the Raviart–Thomas space is nontrivial and technically quite different from that of [25]. The proof is rather lengthy, so we give it separately in the last section.

The rest of the paper is organized as follows. In the next section we introduce the model problem, the quadratic finite element method and the $H(\mathrm{div})$-conforming finite element spaces. Section 3 gives an overview of the equilibrated fluxes of Ainsworth and Oden. In Section 4 we present the main results of this paper: recovery of $H(\mathrm{div})$-conforming flux approximations, the superconvergence result, the postprocessing scheme, and the a posteriori error estimator which achieves both guaranteed upper bound and asymptotic exactness. In Section 5 some numerical results are reported to illustrate the effectiveness of the postprocessing scheme. Finally, Section 6 contains the proof of the superconvergence result presented in Section 4.

2. PRELIMINARIES

2.1. **Model problem.** Let Ω be a bounded polygonal domain in $\mathbb{R}^2$ and consider the second-order self-adjoint elliptic problem

$$\begin{cases} -\operatorname{div}(a(x)\nabla u) + c(x)u = f & \text{in } \Omega, \\ u = u_D & \text{on } \partial\Omega \end{cases} \tag{2.1}$$

for given functions $f \in L^2(\Omega)$ and $u_D \in H^{1/2}(\partial\Omega)$. The coefficient $a(x)$ is a symmetric and uniformly positive definite matrix-valued function and $c(x)$ is a nonnegative function on Ω. The Dirichlet boundary condition is considered only for simplicity, and it is possible to extend subsequent results to more general boundary conditions.

The variational formulation of the problem (2.1) reads as follows: find $u \in H^1(\Omega)$ such that $u|_{\partial\Omega} = u_D$ and

$$B(u, v) = (f, v)_\Omega \qquad \forall v \in H_0^1(\Omega), \tag{2.2}$$

where $(\cdot,\cdot)_G$ denotes the standard L^2 inner product over a subdomain $G \subset \Omega$ and the bilinear form $B(\cdot,\cdot)$ is defined by

$$B(u, v) := (a\nabla u, \nabla v)_\Omega + (cu, v)_\Omega.$$

For later use we define the energy norm of $v \in H^1(\Omega)$ over a subdomain $G \subset \Omega$ as

$$|\!|\!| v |\!|\!|_G := \left(\|a^{1/2}\nabla v\|_{0,G}^2 + \|c^{1/2}v\|_{0,G}^2\right)^{1/2}.$$

2.2. **Finite element method.** Let $\mathcal{T}_h = \{K\}$ be a shape-regular triangulation of Ω with the mesh size $h = \max_{K\in\mathcal{T}_h} h_K$, where h_K is the diameter of K. The set of all vertices of $\mathcal{T}_h$ is denoted by $\mathcal{N}_h = \mathcal{N}_\Omega \cup \mathcal{N}_{\partial\Omega}$, where $\mathcal{N}_\Omega$ and $\mathcal{N}_{\partial\Omega}$ consist of all interior and boundary vertices of $\mathcal{T}_h$, respectively. For a vertex $n \in \mathcal{N}_h$, we denote the set of all elements (resp. edges) of $\mathcal{T}_h$ sharing n by $\mathcal{T}_n$ (resp. $\mathcal{E}_n$) and set $\omega_n = \bigcup_{K\in\mathcal{T}_n} K$. Let $\mathcal{E}_h = \mathcal{E}_\Omega \cup \mathcal{E}_{\partial\Omega}$ be the set of all edges of $\mathcal{T}_h$, where $\mathcal{E}_\Omega$ and $\mathcal{E}_{\partial\Omega}$ consist of all interior and boundary edges of $\mathcal{T}_h$, respectively. For a triangle $K \in \mathcal{T}_h$, let $\mathcal{E}_K$ be the set of three edges of K and $\boldsymbol{n}_K$ the outward unit normal to ∂K.

For simplicity of exposition, we assume that the Dirichlet datum u_D in (2.1) is continuous and piecewise quadratic over $\mathcal{E}_{\partial\Omega}$. This assumption may be removed by including the data oscillation of u_D in subsequent results which is a higher order perturbation if u_D is piecewise smooth over $\mathcal{E}_{\partial\Omega}$.

Let $P_r(K)$ be the space of all polynomials of degree $\le r$ on K and let $u_h \in P_2$ be the continuous piecewise quadratic finite element approximation to the solution u of (2.2) which satisfies $u_h|_{\partial\Omega} = u_D$ and

$$B(u_h, v_h) = (f, v_h)_\Omega \qquad \forall v_h \in P_2 \cap H_0^1(\Omega), \tag{2.3}$$

where P_2 is the quadratic finite element space defined by

$$P_2 := \{v_h \in H^1(\Omega) : v_h|_K \in P_2(K) \ \ \forall K \in \mathcal{T}_h\}.$$

The following optimal H^1-error estimate is well known

$$\|u - u_h\|_{1,\Omega} \le Ch^2\|u\|_{3,\Omega}, \tag{2.4}$$

and by means of the duality argument, one can obtain the L^2-error estimate

$$\|c^{1/2}(u-u_h)\|_{0,\Omega} \le Ch^{2+\epsilon}\|u\|_{3,\Omega}, \tag{2.5}$$

provided that Ω is $(1+\epsilon)$-regular for some $0 < \epsilon \le 1$, namely, the solution u of (2.2) with $u_D = 0$ satisfies the regularity estimate $\|u\|_{1+\epsilon,\Omega} \le C\|f\|_{0,\Omega}$ for every $f \in L^2(\Omega)$. It is well known (cf. [26]) that this regularity estimate holds for bounded polygonal domains (with ϵ depending on the largest interior angle of the domain).

Above and in what follows, the letter C will denote a generic positive constant depending only on the shape-regularity of $\mathcal{T}_h$ and/or the solution u as well as the coefficients $a(x)$ and $c(x)$ of the problem (2.1). Whenever C depends on u, we will explicitly write $C(u)$ to indicate its dependence on u, as in (2.6) below.

The H^1-error estimate (2.4) cannot be improved, except in trivial cases, as we have the following lower bound for quasi-uniform triangulations under mild assumptions on the solution u (see [27, Corollary 3.1])

$$\|\nabla(u-u_h)\|_{0,\Omega} \ge C(u)h^2. \tag{2.6}$$

But, when the triangulation $\mathcal{T}_h$ is structured and the solution u is smooth enough, one can derive a superconvergence result between the finite element solution u_h and some interpolation of u in P_2 defined below.

Let $u_I \in P_2$ be the quadratic interpolation of u which has the same value as u at every vertex of $\mathcal{T}_h$ and the same integral as u over every edge of $\mathcal{T}_h$

$$\int_\gamma (u-u_I)\,ds = 0 \qquad \forall \gamma \in \mathcal{E}_h. \tag{2.7}$$

The following local interpolation error estimate holds for $K \in \mathcal{T}_h$ (cf. [31])

$$\|u-u_I\|_{0,K} + h_K|u-u_I|_{1,K} + h_K^2|u-u_I|_{2,K} \le Ch_K^3|u|_{3,K}. \tag{2.8}$$

We also need some constraints on the structure of the triangulation (cf. [5, 8]).

Condition (α,σ)**:** there exist a partition $\mathcal{T}_h = \mathcal{T}_{1,h} \cup \mathcal{T}_{2,h}$ and positive constants α, σ such that

- every two adjacent triangles of $\mathcal{T}_{1,h}$ form $O(h^{1+\alpha})$-perturbation of a parallelogram.
- $\sum_{K\in\mathcal{T}_{2,h}} |K| = O(h^\sigma)$, where $|K|$ denotes the area of K.

Loosely speaking, this condition means that the triangulation $\mathcal{T}_h$ is nearly uniform except on a small part having area $O(h^\sigma)$. The following superconvergence result was essentially proved in [28] with $\rho = \min(\alpha, \frac{\sigma}{2}, \frac{1}{2})$

$$|\!|\!| u_I - u_h |\!|\!|_\Omega \le Ch^{2+\rho}(\|u\|_{4,\Omega} + |u|_{3,\infty,\Omega}) \tag{2.9}$$

under the assumptions that $\mathcal{T}_h$ satisfies Condition (α,σ) and $u \in H^4(\Omega) \cap W^{3,\infty}(\Omega)$.

Remark 2.1. *Condition* (α,σ) *was extended in* [29] *to Condition* (α,σ,μ) *for adaptive triangulations near corner singularities. Under this condition, the superconvergence result* (2.9) *is proved in terms of the total number of degrees of freedom* N*, instead of the mesh size* h*. We*

believe that the subsequent results of this paper can be extended to triangulations satisfying Condition (α, σ, μ).

2.3. **Raviart–Thomas and Brezzi–Douglas–Marini spaces.** To approximate the flux variable $\boldsymbol{\sigma} := a\nabla u$ in the function space

$$H(\mathrm{div};\Omega) := \{\boldsymbol{\tau} \in (L^2(\Omega))^2 : \mathrm{div}\,\boldsymbol{\tau} \in L^2(\Omega)\},$$

we choose the next-to-lowest Raviart–Thomas and second-order Brezzi–Douglas–Marini spaces defined by

$$\begin{aligned} RT_1 &:= \{\boldsymbol{\tau}_h \in H(\mathrm{div};\Omega) : \boldsymbol{\tau}_h|_K \in RT_1(K) \ \ \forall K \in \mathcal{T}_h\},\\ BDM_2 &:= \{\boldsymbol{\tau}_h \in H(\mathrm{div};\Omega) : \boldsymbol{\tau}_h|_K \in (P_2(K))^2 \ \ \forall K \in \mathcal{T}_h\}, \end{aligned}$$

where

$$RT_1(K) := (P_1(K))^2 + (x_1, x_2)P_1(K).$$

Note that $RT_1 \subsetneq BDM_2$ and

$$\mathrm{div}\, RT_1 = \mathrm{div}\, BDM_2 = \{v_h \in L^2(\Omega) : v_h|_K \in P_1(K) \ \ \forall K \in \mathcal{T}_h\}.$$

The eight degrees of freedom for $\boldsymbol{\tau}_h \in RT_1(K)$ are chosen to be

$$\int_\gamma \boldsymbol{\tau}_h \cdot \boldsymbol{n}_K\, \xi\, ds \quad \text{for } \xi \in P_1(\gamma),\ \gamma \in \mathcal{E}_K \quad \text{and} \quad \int_K \boldsymbol{\tau}_h\, dx, \tag{2.10}$$

where ξ is one of two linear basis functions associated with the vertices of γ.

The Raviart–Thomas interpolation operator $\Pi_h^{RT} : (H^1(\Omega))^2 \cup BDM_2 \to RT_1$ is defined via the degrees of freedom (2.10) by

$$\begin{cases} \displaystyle\int_\gamma \Pi_h^{RT}\boldsymbol{\tau} \cdot \boldsymbol{n}_\gamma\, \xi\, ds = \int_\gamma \boldsymbol{\tau} \cdot \boldsymbol{n}_\gamma\, \xi\, ds & \text{for } \xi \in P_1(\gamma),\ \gamma \in \mathcal{E}_h \\ \displaystyle\int_K \Pi_h^{RT}\boldsymbol{\tau}\, dx = \int_K \boldsymbol{\tau}\, dx & \text{for } K \in \mathcal{T}_h, \end{cases} \tag{2.11}$$

where $\boldsymbol{n}_\gamma$ is a unit normal to γ. By the definition it is easy to verify that

$$\mathrm{div}(\Pi_h^{RT}\boldsymbol{\sigma}) = Q_h^1(\mathrm{div}\,\boldsymbol{\sigma}), \tag{2.12}$$

where $Q_h^1|_K$ is the standard L^2 projection onto $P_1(K)$.

Similarly, the Brezzi–Douglas–Marini interpolation operator $\Pi_h^{BDM} : (H^1(\Omega))^2 \to BDM_2$ can be defined in such a way that

$$\Pi_h^{RT}\Pi_h^{BDM} = \Pi_h^{RT},$$

and the following interpolation error estimates can be derived (cf. [30])

$$\|\boldsymbol{\sigma} - \Pi_h^{RT}\boldsymbol{\sigma}\|_{0,\Omega} \le Ch^2\|\boldsymbol{\sigma}\|_{2,\Omega}, \qquad \|\boldsymbol{\sigma} - \Pi_h^{BDM}\boldsymbol{\sigma}\|_{0,\Omega} \le Ch^3\|\boldsymbol{\sigma}\|_{3,\Omega}. \tag{2.13}$$

3. EQUILIBRATED FLUXES

Guaranteed a posteriori upper bounds on the error $|\!|\!| u-u_h |\!|\!|_\Omega$ can be obtained by applying the hypercircle method of Prager and Synge [10] which requires recovery of a $H(\mathrm{div})$-conforming approximation $\boldsymbol{\sigma}_h \approx \boldsymbol{\sigma} = a\nabla u$ from the finite element approximation $u_h \in P_2$. For this recovery it is convenient to first construct *equilibrated fluxes* $\{g_K \in L^2(\partial K)\}_{K\in\mathcal{T}_h}$, approximating the exact normal fluxes $\{\boldsymbol{\sigma}\cdot\boldsymbol{n}_K|_{\partial K}\}_{K\in\mathcal{T}_h}$, which satisfy the *2nd-order equilibration conditions* for all $K, K' \in \mathcal{T}_h$

$$B_K(u_h, v_h) = (f, v_h)_K + \int_{\partial K} g_K v_h \, ds \qquad \forall v_h \in P_2(K) \tag{3.1}$$

$$g_K + g_{K'} = 0 \qquad \text{on } \partial K \cap \partial K', \tag{3.2}$$

where $B_K(\cdot,\cdot)$ is the restriction of $B(\cdot,\cdot)$ to K

$$B_K(u, v) := (a\nabla u, \nabla v)_K + (cu, v)_K.$$

In [24] the equilibrated flux g_K is taken to be quadratic on each edge of K for quadratic finite elements. Our goal is to recover $\boldsymbol{\sigma}_h \in RT_1$ from g_K via the degrees of freedom (2.10), so it is necessary to compute the integral moments of $g_K|_\gamma$ with respect to linear basis functions associated with the vertices of γ, which will be denoted by

$$\mu^\gamma_{K,n} := \int_\gamma g_K \theta^1_n \, ds.$$

Here $\theta^1_n \in P_1(K)$ is the standard hat function (the subscript n refers to a vertex of γ). We also define the flux moments of a function $w \in H^2(\omega_n)$ by

$$\mu^\gamma_{K,n}(w) := \int_\gamma a\nabla w \cdot \boldsymbol{n}_K \, \theta^1_n \, ds.$$

It was shown in [24, Section 6.7] that the equilibrated flux moments $\{\mu^\gamma_{K,n}\}_{K\in\mathcal{T}_n,\gamma\in\mathcal{E}_n}$ associated with each vertex $n \in \mathcal{N}_h$ may be determined by solving a small local problem over the patch ω_n. In the following we give a brief description of some notation and results about $\{\mu^\gamma_{K,n}\}_{K\in\mathcal{T}_n,\gamma\in\mathcal{E}_n}$ which are mostly taken from [4, Subsection 6.1].

Fix a vertex $n \in \mathcal{N}_h$ and let N be the number of elements in $\mathcal{T}_n$ (depending on n). The elements in $\mathcal{T}_n$ are numbered clockwise as $K_1, K_2, \cdots, K_N$ and the edges in $\mathcal{E}_n$ as $\gamma_1, \gamma_2, \cdots, \gamma_{N+1}$ in such a way that $\gamma_i = \partial K_{i-1} \cap \partial K_i$ for $2 \le i \le N$. Note that $\gamma_1 = \gamma_{N+1} = \partial K_1 \cap \partial K_N$ if $n \in \mathcal{N}_\Omega$, but γ_1 and γ_{N+1} are different boundary edges if $n \in \mathcal{N}_{\partial\Omega}$. For brevity, we set

$$\mu^\gamma_{i,n} = \mu^\gamma_{K_i,n}, \qquad \mu^\gamma_{i,n}(w) = \mu^\gamma_{K_i,n}(w) \qquad (1 \le i \le N)$$

and define the following $2N \times 1$ vectors of flux moments associated with vertex n

$$\boldsymbol{b}_n := \left[\ \mu^{\gamma_1}_{1,n}, \quad \cdots, \quad \mu^{\gamma_N}_{N,n}, \qquad \mu^{\gamma_2}_{1,n}, \quad \cdots, \quad \mu^{\gamma_{N+1}}_{N,n}\ \right]^T,$$

$$\boldsymbol{b}_n(w) := \left[\ \mu^{\gamma_1}_{1,n}(w), \quad \cdots, \quad \mu^{\gamma_N}_{N,n}(w), \qquad \mu^{\gamma_2}_{1,n}(w), \quad \cdots, \qquad \mu^{\gamma_{N+1}}_{N,n}(w)\ \right]^T.$$

Then the equilibration conditions (3.1)–(3.2) with $v_h = \theta_n^1$ applied to $K_1, K_2, \cdots, K_N$ lead to the following system of $2N$ linear equations for the vector $\boldsymbol{b}_n$ (containing $2N$ unknowns)

$$\mu_{i,n}^{\gamma_i} + \mu_{i,n}^{\gamma_{i+1}} = \Delta_i(u_h) \qquad (1 \le i \le N) \tag{3.3}$$

$$\mu_{1,n}^{\gamma_1} + \mu_{N,n}^{\gamma_{N+1}} = \sum_{i=1}^{N} \Delta_i(u_h) \tag{3.4}$$

$$\mu_{i-1,n}^{\gamma_i} + \mu_{i,n}^{\gamma_i} = 0 \qquad (2 \le i \le N), \tag{3.5}$$

where

$$\Delta_i(w) := B_{K_i}(w, \theta_n^1) - (f, \theta_n^1)_{K_i}.$$

The equation (3.4) is actually redundant as it can be obtained from (3.3) and (3.5). Hence the linear system (3.3)–(3.5) is valid for all $n \in \mathcal{N}_h$.

To write (3.3)–(3.5) in matrix-vector form, we introduce the following permutation of the $N \times N$ identity matrix I_N

$$J_N := \begin{bmatrix} 0 & 0 & \cdots & 0 & 1 \\ 1 & 0 & \cdots & 0 & 0 \\ \vdots & \vdots & & \vdots & \vdots \\ 0 & 0 & \cdots & 1 & 0 \end{bmatrix}$$

and the $N \times 1$ and $(N-1) \times 1$ vectors consisting of ones and zeros

$$\mathbf{1}_N := \begin{bmatrix} 1 & 1 & \cdots & 1 \end{bmatrix}^T, \qquad \mathbf{0}_{N-1} := \begin{bmatrix} 0 & 0 & \cdots & 0 \end{bmatrix}^T.$$

Then the linear system (3.3)–(3.5) is equal to

$$A_N \boldsymbol{b}_n = \begin{bmatrix} \boldsymbol{y}_n(u_h) \\ \sum_{i=1}^N \Delta_i(u_h) \\ \mathbf{0}_{N-1} \end{bmatrix},$$

where

$$A_N := \begin{bmatrix} I_N & I_N \\ I_N & J_N \end{bmatrix}, \qquad \boldsymbol{y}_n(w) := \begin{bmatrix} \Delta_1(w), & \Delta_2(w), & \cdots, & \Delta_N(w) \end{bmatrix}^T.$$

Since the equation (3.4) is redundant and the null space of A_N is the one-dimensional space spanned by $\boldsymbol{\nu}_N := \begin{bmatrix} \mathbf{1}_N \\ -\mathbf{1}_N \end{bmatrix}$ (cf. [4]), this system has a one-parameter family of solutions among which we choose the solution minimizing the quadratic functional

$$|\boldsymbol{b}_n - \boldsymbol{b}_n(u_h)|^2 = \sum_{K \in \mathcal{T}_n} \sum_{\gamma \in \mathcal{E}_n \cap \mathcal{E}_K} \left(\mu_{K,n}^{\gamma} - \mu_{K,n}^{\gamma}(u_h)\right)^2.$$

It was shown in [4] that this choice gives the solution $\boldsymbol{b}_n$ which uniquely solves the $(2N+1)\times 2N$ (augmented) matrix system

$$\begin{bmatrix} A_N \\ \boldsymbol{\nu}_N^T \end{bmatrix} \boldsymbol{b}_n = \begin{bmatrix} \boldsymbol{y}_n(u_h) \\ \sum_{i=1}^N \Delta_i(u_h) \\ \mathbf{0}_{N-1} \\ \boldsymbol{\nu}_N^T \boldsymbol{b}_n(u_h) \end{bmatrix}. \tag{3.6}$$

We can also deduce the following stability result from that of [4] when the matrix system (3.6) has a more general right-hand side.

Lemma 3.1. *For all* $\boldsymbol{y} = \begin{bmatrix} y_1 & y_2 & \cdots & y_N \end{bmatrix}^T$ *and* $z \in \mathbb{R}$, *the* $(2N+1)\times 2N$ *matrix system*

$$\begin{bmatrix} A_N \\ \boldsymbol{\nu}_N^T \end{bmatrix} \boldsymbol{x} = \begin{bmatrix} \boldsymbol{y} \\ \sum_{i=1}^N y_i \\ \mathbf{0}_{N-1} \\ z \end{bmatrix} \tag{3.7}$$

has a unique solution $\boldsymbol{x} \in \mathbb{R}^{2N}$ *which satisfies*

$$|\boldsymbol{x}| \le C(|\boldsymbol{y}| + |z|),$$

where the constant C *depends only on* N.

Remark 3.2. *Let us briefly describe a solution of the linear system* (3.3)–(3.5) *for a boundary vertex* n *in the case of the mixed boundary condition*

$$u|_{\partial\Omega\setminus\Gamma} = u_D \qquad \text{and} \qquad a\nabla u\cdot \boldsymbol{n}|_\Gamma = g_\Gamma, \tag{3.8}$$

where $\boldsymbol{n}$ *is the outward unit normal to* $\partial\Omega$ *and every* $\gamma \in \mathcal{E}_{\partial\Omega}$ *lies in either* Γ *or* $\partial\Omega\setminus\Gamma$. *If* $\gamma_1 \subset \Gamma$, *then we set*

$$\mu_{1,n}^{\gamma_1} = \int_{\gamma_1} g_\Gamma \theta_n^1 \, ds. \tag{3.9}$$

Since the linear system (3.3)–(3.5) *is valid for all* $n \in \mathcal{N}_h$ *and its null space is one-dimensional, it has a unique solution once* $\mu_{1,n}^{\gamma_1}$ *is chosen as* (3.9). *If* $\gamma_1 \cup \gamma_{N+1} \subset \Gamma$, *we further obtain*

$$\sum_{i=1}^N \Delta_i(u_h) = B(u_h,\theta_n^1) - (f,\theta_n^1)_\Omega = \int_{\gamma_1} g_\Gamma\theta_n^1\,ds + \int_{\gamma_{N+1}} g_\Gamma\theta_n^1\,ds,$$

which gives by (3.4) *and* (3.9)

$$\mu_{N,n}^{\gamma_{N+1}} = \int_{\gamma_{N+1}} g_\Gamma\theta_n^1\,ds. \tag{3.10}$$

Analogous results are obtained in the case that $\gamma_{N+1} \subset \Gamma$. *In other words, depending on whether* $\gamma_1 \subset \Gamma$ *or* $\gamma_{N+1}\subset\Gamma$, *we fix* $\mu_{1,n}^{\gamma_1}$ *by* (3.9) *or* $\mu_{N,n}^{\gamma_{N+1}}$ *by* (3.10) *but only one of them*

when $\gamma_1 \cup \gamma_{N+1} \subset \Gamma$ (*the other one automatically satisfies* (3.9) *or* (3.10) *by solving* (3.3)–(3.5)).

4. MAIN RESULTS

In this section we present a recovery method of $H(\mathrm{div})$-conforming flux approximations from the equilibrated flux moments $\{\mu^{\gamma}_{K,n}\}$ and derive guaranteed a posteriori upper bounds on the error $|\!|\!| u - u_h |\!|\!|_{\Omega}$ by applying the hypercircle method of Prager and Synge [10]. The overall framework follows the approach of [25] given for linear finite elements. The key result is Theorem 4.2 which enables us to construct a superconvergent flux approximation and a posteriori error estimator which achieves both guaranteed upper bound and asymptotic exactness.

4.1. **Recovery of flux approximation in RT_1 and superconvergence.** We recover a flux approximation $\boldsymbol{\sigma}_h|_K \in RT_1(K)$ on each element $K \in \mathcal{T}_h$ by specifying its degrees of freedom (2.10) as

$$\begin{cases} \displaystyle\int_{\gamma} \boldsymbol{\sigma}_h|_K \cdot \boldsymbol{n}_K \, \xi \, ds = \int_{\gamma} g_K \xi \, ds \qquad \text{for } \xi \in P_1(\gamma),\ \gamma \in \mathcal{E}_K \\ \displaystyle\int_K \boldsymbol{\sigma}_h \, dx = \int_K a \nabla u_h \, dx. \end{cases} \tag{4.1}$$

By taking $\xi = \theta^1_n$, we immediately see that what is actually needed in computing $\boldsymbol{\sigma}_h|_K$ are the equilibrated flux moments $\{\mu^{\gamma}_{K,n}\}$, not the flux function g_K itself.

The equilibration condition (3.2) implies that $\boldsymbol{\sigma}_h$ has continuous normal components across the edges of $\mathcal{T}_h$ and so $\boldsymbol{\sigma}_h \in RT_1$, although it is computed locally on each element of $\mathcal{T}_h$. From (3.1) and (4.1), we also obtain for all $K \in \mathcal{T}_h$ and $v_h \in P_1(K)$

$$\begin{aligned} (\mathrm{div}\, \boldsymbol{\sigma}_h + f - cu_h, v_h)_K &= \int_{\partial K} \boldsymbol{\sigma}_h \cdot \boldsymbol{n}_K \, v_h \, ds - (\boldsymbol{\sigma}_h, \nabla v_h)_K + (f - cu_h, v_h)_K \\ &= \int_{\partial K} g_K v_h \, ds - (a \nabla u_h, \nabla v_h)_K + (f - cu_h, v_h)_K \\ &= (f, v_h)_K - B_K(u_h, v_h) + \int_{\partial K} g_K v_h \, ds = 0, \end{aligned}$$

which gives the local conservation law

$$\mathrm{div}\, \boldsymbol{\sigma}_h = -Q^1_h(f - cu_h). \tag{4.2}$$

Moreover, we can show that $\boldsymbol{\sigma}_h$ has optimal order of convergence in the L^2 norm.

Theorem 4.1. *Let* $\boldsymbol{\sigma}_h \in RT_1$ *be defined by* (4.1) *and assume that* $u \in H^3(\Omega)$. *Then there exists a constant* $C > 0$ *such that*

$$\|\boldsymbol{\sigma} - \boldsymbol{\sigma}_h\|_{0,\Omega} \le Ch^2 \|u\|_{3,\Omega}.$$

In general we cannot expect a better order of convergence than stated in the above theorem, since $RT_1(K) \subsetneq (\mathbb{P}_2(K))^2$. But, under additional conditions on the structure of the triangulation and the regularity of the exact solution, it is possible to prove the following super-closeness between $\boldsymbol{\sigma}_h$ and $\Pi_h^{RT}\boldsymbol{\sigma}$.

Theorem 4.2. *Let $\boldsymbol{\sigma}_h \in RT_1$ be defined by* (4.1) *and assume that the triangulation $\mathcal{T}_h$ satisfies Condition (α, σ) and $u \in H^4(\Omega) \cap W^{3,\infty}(\Omega)$. If the mesh size h is sufficiently small, then there exists a constant $C > 0$ such that*

$$\|\boldsymbol{\sigma}_h - \Pi_h^{RT}\boldsymbol{\sigma}\|_{0,\Omega} \le Ch^{2+\rho}(\|u\|_{4,\Omega} + |u|_{3,\infty,\Omega})$$

with $\rho = \min(\alpha, \frac{\sigma}{2}, \frac{1}{2})$.

The proofs of Theorems 4.1–4.2 are quite involved and postponed to Section 6.

4.2. **Recovery of superconvergent flux approximation in BDM_2.** Following the approach of [25] (see also [15, 16, 19]), we now attempt to improve the accuracy of $\boldsymbol{\sigma}_h \in RT_1$ by adding to it some $\mathbf{curl}\,\psi_h \in BDM_2$, where $\mathbf{curl}\,v = \big(\frac{\partial v}{\partial x_2}, -\frac{\partial v}{\partial x_1}\big)$, which minimizes the L^2 error of the flux approximation. The scalar function ψ_h will be found in the global space of cubic bump functions

$$P_3^0 := \{\varphi_h \in H^1(\Omega) : \varphi_h|_K \in P_3^0(K) \ \ \forall K \in \mathcal{T}_h\},$$

where

$$P_3^0(K) := \{v \in P_3(K) : v = 0 \text{ at vertices and midpoints of edges of } K\}.$$

Note that P_3^0 acts as a *correction* space for RT_1 in BDM_2 via the hierarchical splitting

$$BDM_2 = RT_1 \oplus \mathbf{curl}\, P_3^0$$

which follows directly from Lemma 4.3 given below. We remark that the local correction space $P_3^0(K)$ was employed in [3] to define an asymptotically exact error estimator of the Bank–Weiser type for quadratic finite element methods.

Lemma 4.3. *For any $\boldsymbol{\tau}_h \in BDM_2$, there exists a function $\varphi_h \in P_3^0$ such that*

$$\boldsymbol{\tau}_h = \Pi_h^{RT}\boldsymbol{\tau}_h + \mathbf{curl}\,\varphi_h.$$

Proof. By (2.12) we have $\operatorname{div}(\boldsymbol{\tau}_h - \Pi_h^{RT}\boldsymbol{\tau}_h) = 0$, and so there exists a continuous piecewise cubic function φ_h such that (see, for example, [30])

$$\boldsymbol{\tau}_h - \Pi_h^{RT}\boldsymbol{\tau}_h = \mathbf{curl}\,\varphi_h.$$

From (2.11) it follows that for all $\xi \in P_1(\gamma)$ and $\gamma \in \mathcal{E}_h$,

$$\int_\gamma \frac{\partial \varphi_h}{\partial t_\gamma}\,\xi\,ds = \int_\gamma (\boldsymbol{\tau}_h - \Pi_h^{RT}\boldsymbol{\tau}_h)\cdot \boldsymbol{n}_\gamma\,\xi\,ds = 0,$$

where $\frac{\partial w}{\partial t_\gamma} = \nabla w \cdot \boldsymbol{t}_\gamma$ denotes the tangential derivative of w along γ. By taking $\xi = 1$, we may assume that $\varphi_h = 0$ at vertices of $\mathcal{T}_h$. Then the integration by parts gives

$$\int_\gamma \varphi_h \frac{\partial \xi}{\partial t_\gamma}\,ds = -\int_\gamma \frac{\partial \varphi_h}{\partial t_\gamma}\,\xi\,ds = 0,$$

which implies that $\int_\gamma \varphi_h\, ds = 0$ and so $\varphi_h = 0$ at the midpoint of γ. Hence it is proved that $\varphi_h \in P_3^0$. □

We observe that the best function $\psi_h \in P_3^0$ for which $\boldsymbol{\sigma}_h + \mathbf{curl}\,\psi_h \approx \boldsymbol{\sigma}$ would be the solution of the global minimization problem

$$\min_{\varphi_h \in P_3^0} \|a^{-1/2}(\boldsymbol{\sigma}_h + \mathbf{curl}\,\varphi_h - a\nabla u)\|_{0,\Omega}. \tag{4.3}$$

By the assumption $u_h|_{\partial\Omega} = u_D = u|_{\partial\Omega}$, it can be shown that ψ_h is also the solution of the minimization problem (see [25, Lemma 4.1] for linear finite element methods)

$$\min_{\varphi_h \in P_3^0} \|a^{-1/2}(\boldsymbol{\sigma}_h + \mathbf{curl}\,\varphi_h - a\nabla u_h)\|_{0,\Omega} \tag{4.4}$$

which is equivalent to the following variational problem: find $\psi_h \in P_3^0$ such that

$$(a^{-1}\,\mathbf{curl}\,\psi_h, \mathbf{curl}\,\varphi_h)_\Omega = -(a^{-1}(\boldsymbol{\sigma}_h - a\nabla u_h), \mathbf{curl}\,\varphi_h)_\Omega \qquad \forall \varphi_h \in P_3^0. \tag{4.5}$$

In other words, the solution of (4.3) can be computed from u_h by solving (4.5).

Remark 4.4. *Clearly, the matrix system of* (4.5) *is symmetric and positive definite. Although it is global in nature, the choice of the trial space P_3^0 makes it locally equivalent to a scaled mass matrix and hence well-conditioned* (*at least on quasi-uniform triangulations*)*, as mentioned in* [25] *for linear finite element methods. Numerical experiments indicate that even a few cg iterations for* (4.5) *would suffice to get satisfactory results.*

Remark 4.5. *In the case of the mixed boundary condition* (3.8)*, we further impose the constraint $\varphi_h|_\Gamma = 0$ on the correction space P_3^0, which implies that $\mathbf{curl}\,\varphi_h \cdot \boldsymbol{n}|_\Gamma = 0$ for all $\varphi_h \in P_3^0$ and so $(\boldsymbol{\sigma}_h + \mathbf{curl}\,\psi_h)\cdot\boldsymbol{n} = \boldsymbol{\sigma}_h \cdot \boldsymbol{n}$ on Γ.*

Now using the superconvergence result of Theorem 4.2, we prove that $\boldsymbol{\sigma}_h + \mathbf{curl}\,\psi_h$ may converge to $\boldsymbol{\sigma} = a\nabla u$ at a higher order than $\boldsymbol{\sigma}_h$ and $a\nabla u_h$ shown in Theorem 4.1 and (2.4).

Theorem 4.6. *Under the assumptions of Theorem* 4.2*, there exists a constant $C > 0$ such that*

$$\|a^{-1/2}(\boldsymbol{\sigma}_h + \mathbf{curl}\,\psi_h - \boldsymbol{\sigma})\|_{0,\Omega} \le Ch^{2+\rho}(\|u\|_{4,\Omega} + |u|_{3,\infty,\Omega})$$

with $\rho = \min(\alpha, \frac{\sigma}{2}, \frac{1}{2})$.

Proof. The proof is the same as that of [25, Theorem 4.2] for linear finite element methods. We include it here for the reader's convenience.

Applying Lemma 4.3 to $\boldsymbol{\tau}_h = \Pi_h^{BDM}\boldsymbol{\sigma}$ and using the property $\Pi_h^{RT}\Pi_h^{BDM} = \Pi_h^{RT}$, we have for some $\varphi_h \in P_3^0$

$$\Pi_h^{BDM}\boldsymbol{\sigma} - \Pi_h^{RT}\boldsymbol{\sigma} = \mathbf{curl}\,\varphi_h.$$

Since $\psi_h \in P_3^0$ is the solution of the minimization problem (4.3), it follows that

$$\begin{aligned}\|a^{-1/2}(\boldsymbol{\sigma}_h + \mathbf{curl}\,\psi_h - \boldsymbol{\sigma})\|_{0,\Omega} &\le \|a^{-1/2}(\boldsymbol{\sigma}_h + \mathbf{curl}\,\varphi_h - \boldsymbol{\sigma})\|_{0,\Omega} \\ &\le C(\|\boldsymbol{\sigma}_h - \Pi_h^{RT}\boldsymbol{\sigma}\|_{0,\Omega} + \|\Pi_h^{BDM}\boldsymbol{\sigma} - \boldsymbol{\sigma}\|_{0,\Omega}).\end{aligned}$$

The proof is completed by invoking Theorem 4.2 and the interpolation error estimate (2.13). □

4.3. **Guaranteed and asymptotically exact a posteriori error bound.** Since the local conservation law (4.2) gives

$$\operatorname{div}(\boldsymbol{\sigma}_h + \mathbf{curl}\,\psi_h) = \operatorname{div}\boldsymbol{\sigma}_h = -Q_h^1(f - cu_h),$$

we can apply the hypercircle method of Prager and Synge [10] to obtain the following *guaranteed a posteriori error bound* (see, for example, [11, 13, 16, 18, 21])

$$\begin{aligned}\|\!|u - u_h|\!\|_\Omega \le \eta := \Big\{ \sum_{K\in\mathcal{T}_h} \Big(&\|a^{-1/2}(\boldsymbol{\sigma}_h + \mathbf{curl}\,\psi_h - a\nabla u_h)\|_{0,K} \\ &+ \frac{h_K}{\pi\lambda_K^{1/2}} \|\operatorname{div}\boldsymbol{\sigma}_h + f - cu_h\|_{0,K} \Big)^2 \Big\}^{1/2}, \quad (4.6)\end{aligned}$$

where $\lambda_K > 0$ is a uniform lower bound on the smallest eigenvalues of $a(x)|_K$, i.e.,

$$z^T a(x) z \ge \lambda_K z^T z \qquad \forall z \in \mathbb{R}^2,\ x \in K.$$

Besides, by virtue of Theorem 4.6, we can show that the error bound η is *asymptotically exact* under stronger conditions on the solution u and the triangulation $\mathcal{T}_h$. Since the proof is essentially the same as that of [25, Theorem 4.3], we only give details for the nontrivial part.

Theorem 4.7. *Assume that c and f are piecewise smooth over $\mathcal{T}_h$. Then, under the assumptions of Theorem* 4.2*, we have*

$$\|a^{1/2}\nabla(u - u_h)\|_{0,\Omega} = \eta + O\big(C(u)h^{2+\rho}\big)$$

with $\rho = \min(\alpha, \frac{\sigma}{2}, \frac{1}{2})$. Moreover, if the L^2-error estimate (2.5) *and the non-degeneracy condition* (2.6) *hold, then we have*

$$\left| \frac{\eta}{\|\!|u - u_h|\!\|_\Omega} - 1 \right| \le C(u) h^{\min(\rho,\epsilon)}.$$

Proof. The nontrivial part is to show that the second term of η is of the order $O(h^3)$. Using the local conservation law (4.2) and the estimate $\|v - Q_h^1 v\|_{0,K} \le C h_K^r |v|_{r,K}$ for $r = 1, 2$, we obtain

$$\begin{aligned}\|\operatorname{div}\boldsymbol{\sigma}_h + f - cu_h\|_{0,K} &= \|f - cu_h - Q_h^1(f - cu_h)\|_{0,K} \\ &\le \|f - cu - Q_h^1(f - cu)\|_{0,K} \\ &\qquad + \|c(u - u_h) - Q_h^1(c(u - u_h))\|_{0,K} \\ &\le C h_K^2 |f - cu|_{2,K} + C h_K \|u - u_h\|_{1,K}.\end{aligned}$$

Hence it follows by (2.4) that

$$\Big\{ \sum_{K\in\mathcal{T}_h} \frac{h_K^2}{\pi^2\lambda_K} \|\operatorname{div}\boldsymbol{\sigma}_h + f - cu_h\|_{0,K}^2 \Big\}^{1/2} \le C(u)h^3,$$

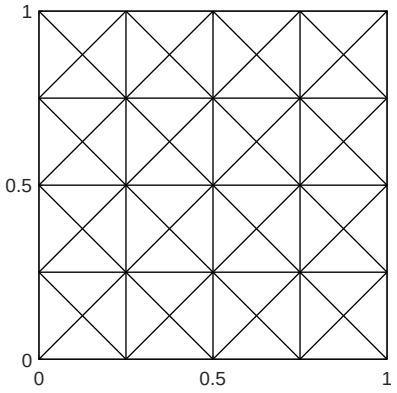

FIGURE 1. 4×4 criss-cross triangulation with the mesh size $h = 1/4$ in Example 1

which proves the desired assertion. □

Remark 4.8. *The results of this section are extended without modification to the case of the mixed boundary condition* (3.8) *if* $\boldsymbol{\sigma}_h \cdot \boldsymbol{n}|_\Gamma = g_\Gamma$*, i.e., the Neumann datum* g_Γ *is piecewise linear over* Γ*. Otherwise, it is necessary to include the data oscillation of* g_Γ *which is a higher order perturbation if* g_Γ *is piecewise smooth.*

5. NUMERICAL RESULTS

To verify the effectiveness of superconvergent flux recovery in BDM_2 presented in the previous section, we carry out some numerical experiments for two examples.

Example 1. Let $\Omega = (0,1)^2$ and consider the problem

$$-\Delta u + u = f \quad \text{in } \Omega$$

with the exact solution chosen to be

$$u(x,y) = \sin(2\pi x)\sin(\pi y) + x^2 + xy + 2y^2.$$

Since u is quadratic on $\partial\Omega$, the finite element solution $u_h \in P_2$ exactly satisfies the Dirichlet boundary condition imposed on $\partial\Omega$.

First we consider a sequence of triangulations generated through successive refinements of the initial 4×4 criss-cross triangulation displayed in Fig. 1. Each refinement divides every triangle of a triangulation into four equal subtriangles by connecting the midpoints of three edges (which is usually called red refinement). These triangulations satisfy Condition (α, σ) with $\alpha = \infty$ and $\sigma = 1$.

In Table 1 we report the L^2 errors of the recovered flux approximations $\boldsymbol{\sigma}_h \in RT_1$ and $\boldsymbol{\sigma}_h^* := \boldsymbol{\sigma}_h + \mathbf{curl}\,\psi_h \in BDM_2$, with $\psi_h \in P_3^0$ computed by solving (4.5) exactly. The convergence orders are numerically calculated from the errors on two consecutive triangulations. It is clearly

TABLE 1. L^2 errors of the flux approximations for uniformly refined triangulations in Example 1

$1/h$	$\|\boldsymbol{\sigma}-\boldsymbol{\sigma}_h\|_{0,\Omega}$	Order	$\|\boldsymbol{\sigma}_h-\Pi_h^{RT}\boldsymbol{\sigma}\|_{0,\Omega}$	Order	$\|\boldsymbol{\sigma}-\boldsymbol{\sigma}_h^*\|_{0,\Omega}$	Order
4	1.6133e–1	—	6.0994e–2	—	6.6788e–2	—
8	3.6589e–2	2.1405	9.3482e–3	2.7059	9.5769e–3	2.8020
16	8.7726e–3	2.0604	1.3353e–3	2.8075	1.3486e–3	2.8281
32	2.1651e–3	2.0185	1.9870e–4	2.7486	2.0018e–4	2.7521
64	5.3918e–4	2.0056	3.1294e–5	2.6666	3.1433e–5	2.6710
128	1.3462e–4	2.0019	5.1637e–6	2.5994	5.1703e–6	2.6039
256	3.3639e–5	2.0007	8.7874e–7	2.5549	8.7784e–7	2.5582

TABLE 2. Effectivity indices of the error estimator η_k ($k = 0, 1, 3, \infty$) for uniformly refined triangulations in Example 1

$1/h$	I_0	I_1	I_3	I_∞
4	1.6546	1.4799	1.4379	1.4378
8	1.3863	1.2352	1.1965	1.1963
16	1.2702	1.1292	1.0925	1.0923
32	1.2177	1.0805	1.0450	1.0448
64	1.1929	1.0571	1.0223	1.0221
128	1.1808	1.0457	1.0111	1.0110
256	1.1749	1.0401	1.0056	1.0055

observed that $\boldsymbol{\sigma}_h$ is super-close to $\Pi_h^{RT}\boldsymbol{\sigma}$ as proved in Theorem 4.2 and the postprocessing scheme (4.4) improves the convergence order of $\boldsymbol{\sigma}_h$ as predicted by Theorem 4.6.

To study the effect of applying a few iterations of the conjugate gradient (cg) method for $\psi_h \in P_3^0$, we solve (4.5) by (unpreconditioned) k cg iterations starting with the zero vector. For $k = 0$ we have $\psi_h = 0$, and $k = \infty$ means that ψ_h is the exact solution of (4.5). The resulting error estimator in (4.6) is denoted by η_k. Table 2 reports the values of the effectivity index $I_k := \eta_k / |\!|\!| u - u_h |\!|\!|_\Omega$ for $k = 0, 1, 3, \infty$. It is observed that even a single cg iteration remarkably improves the effectivity index and $k = 3$ cg iterations yield almost the same results as $k = \infty$. Moreover, we have $|I_\infty - 1| = O(h)$, which is better than predicted by Theorem 4.7.

Next we consider a sequence of $n \times n$ criss-cross triangulations with the mesh size $h = 1/2^n$ (see Fig. 1 for $n = 2$) which do not satisfy Condition (α, σ) for any $\sigma > 0$. The numerical results are reported in Tables 3–4, which show that the super-closeness between $\boldsymbol{\sigma}_h$ and $\Pi_h^{RT}\boldsymbol{\sigma}$ is lost and the accuracy of $\boldsymbol{\sigma}_h^*$ is only slightly better than $\boldsymbol{\sigma}_h$ (with no improvement in the convergence order). Nonetheless, the postprocessing scheme (4.4) seems very effective as it

TABLE 3. L^2 errors of the flux approximations for criss-cross triangulations in Example 1

$1/h$	$\|\boldsymbol{\sigma}-\boldsymbol{\sigma}_h\|_{0,\Omega}$	Order	$\|\boldsymbol{\sigma}_h-\Pi_h^{RT}\boldsymbol{\sigma}\|_{0,\Omega}$	Order	$\|\boldsymbol{\sigma}-\boldsymbol{\sigma}_h^*\|_{0,\Omega}$	Order
4	1.6133e–1	—	6.0994e-2	—	6.6788e–2	—
8	4.2015e–2	1.9410	1.8331e-2	1.7344	1.6420e–2	2.0241
16	1.0629e–2	1.9829	4.8080e-3	1.9308	4.0920e–3	2.0046
32	2.6653e–3	1.9956	1.2166e-3	1.9825	1.0223e–3	2.0010
64	6.6685e–4	1.9989	3.0509e-4	1.9956	2.5553e–4	2.0002
128	1.6674e–4	1.9997	7.6330e-5	1.9989	6.3879e–5	2.0001
256	4.1688e–5	1.9999	1.9086e-5	1.9997	1.5970e–5	2.0000

TABLE 4. Effectivity indices of the error estimator η_k ($k = 0, 1, 3, \infty$) for criss-cross triangulations in Example 1

$1/h$	I_0	I_1	I_3	I_∞
4	1.6546	1.4799	1.4379	1.4378
8	1.4527	1.2603	1.2210	1.2209
16	1.3654	1.1679	1.1313	1.1313
32	1.3228	1.1231	1.0883	1.0883
64	1.3015	1.1008	1.0670	1.0670
128	1.2909	1.0896	1.0564	1.0564
256	1.2855	1.0840	1.0511	1.0511

makes the effectivity index quite close to one as $h \to 0$, although I_∞ does not seem to tend to one.

Example 2. In the second example we consider the following problem from [15]

$$-\Delta u = 1 \quad \text{in } \Omega = (-1,1)^2 \setminus ([0,1] \times [-1,0])$$

with the homogeneous Dirichlet boundary condition $u|_{\partial\Omega} = 0$. Since the exact solution u is not known, it is not possible to calculate the L^2 errors of the flux approximations. But, by using the numerical approximation $\|\nabla u\|_{0,\Omega}^2 = 0.214075802680976\cdots$ available from [15], the energy-norm error $|||u - u_h|||_\Omega$ can be calculated by

$$|||u-u_h|||_\Omega^2 = \|\nabla(u-u_h)\|_{0,\Omega}^2 = \|\nabla u\|_{0,\Omega}^2 - \|\nabla u_h\|_{0,\Omega}^2.$$

First we consider a sequence of uniform regular triangulations with the mesh size $h = \sqrt{2}/2^n$ satisfying Condition (α, σ) with $\alpha = \sigma = \infty$. These triangulations are generated by successive red refinements of the coarse triangulation (with the mesh size $h = \sqrt{2}/2$) shown in the left of Fig. 2. In Table 5 we report the values of the effectivity index I_k ($k = 0, 1, 3, \infty$).

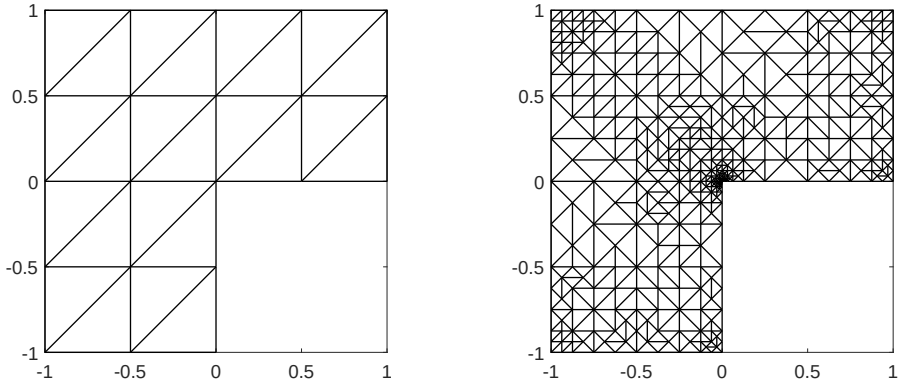

FIGURE 2. Initial triangulation with 65 dofs (left) and adaptive triangulation with 1647 dofs after 10 refinements (right) for Example 2

TABLE 5. Effectivity indices of the error estimator η_k ($k = 0, 1, 3, \infty$) for uniform regular triangulations in Example 2

$\sqrt{2}/h$	I_0	I_1	I_3	I_∞
4	1.9427	1.4795	1.3710	1.3706
8	2.0124	1.5297	1.4181	1.4177
16	2.0287	1.5415	1.4291	1.4287
32	2.0318	1.5439	1.4312	1.4308
64	2.0323	1.5444	1.4316	1.4312
128	2.0324	1.5445	1.4316	1.4312
256	2.0324	1.5445	1.4317	1.4312

Numerical results show that $\|\!|u - u_h|\!|_\Omega = O(h^{0.6667})$, and so there is a lack of regularity of the solution u. This implies that we cannot expect the error estimator η_∞ to be asymptotically exact, as observed in Table 5. It is noteworthy that the postprocessing scheme (4.4) significantly improves the effectivity index even when the exact solution is not regular enough.

Next we apply adaptive mesh refinement guided by the error estimator η_0 to generate a sequence of triangulation from the initial triangulation in the left of Fig. 2. One of these adaptive triangulations is shown in the right of Fig. 2, from which one can see that the mesh refinement is concentrated near the re-entrant corner of Ω. We remark that the least-squares fitting gives almost optimal convergence order $\|\!|u - u_h|\!|_\Omega = O(N^{-1.0496})$ with respect to the number of degrees of freedom $N = \dim P_2$. This implies that the singularity of u is well resolved by the adaptive triangulations generate above.

Table 6 reports the values of the effectivity index I_k ($k = 0, 1, 3, \infty$) for some selected subset of adaptive triangulations. Unlike uniform regular triangulations, it is observed that

TABLE 6. Effectivity indices of the error estimator η_k ($k = 0, 1, 3, \infty$) for adaptive triangulations in Example 2

N	I_0	I_1	I_3	I_∞
65	1.7672	1.3460	1.2505	1.2501
227	1.8006	1.3638	1.2494	1.2487
401	1.6242	1.2584	1.1452	1.1447
599	1.5720	1.2032	1.0851	1.0845
1097	1.5532	1.1898	1.0691	1.0686
1647	1.5042	1.1565	1.0399	1.0394
3093	1.4959	1.1470	1.0319	1.0314
5153	1.4826	1.1415	1.0240	1.0234
9459	1.4703	1.1300	1.0184	1.0178
17209	1.4652	1.1278	1.0160	1.0154
31509	1.4588	1.1220	1.0136	1.0131
57549	1.4539	1.1221	1.0120	1.0115
107591	1.4510	1.1174	1.0116	1.0111
192021	1.4502	1.1223	1.0132	1.0127
361127	1.4613	1.1311	1.0221	1.0216
655417	1.4877	1.1521	1.0424	1.0419

the effectivity index stays very close to one by using the postprocessing scheme (4.4). This is possibly due to the fact that the solution u looks "regular" when its singularity is resolved by adaptive triangulations, but more investigation is needed to give a rigorous analysis of this observation (cf. Remark 2.1).

6. PROOF OF THEOREMS 4.1–4.2

In this section we prove Theorems 4.1–4.2 through a series of lemmas. Recall that $u_h \in P_2$ is the finite element solution of (2.3) and $\boldsymbol{\sigma}_h \in RT_1$ is computed on each element $K \in \mathcal{T}_h$ by (4.1). See Section 3 for notation and results about flux moments used below. For an edge $\gamma \in \mathcal{E}_h$, we also use the notation $\mathcal{N}_\gamma$ to denote the set of two vertices of γ.

Lemma 6.1. *We have for all $K \in \mathcal{T}_h$*

$$\|\boldsymbol{\sigma}_h - \Pi_h^{RT}\boldsymbol{\sigma}\|_{0,K} \le C\bigg(h_K^3|u|_{3,K} + \|\nabla(u_I - u_h)\|_{0,K} + \sum_{\gamma\in\mathcal{E}_K}\sum_{n\in\mathcal{N}_\gamma}\big|\mu_{K,n}^\gamma - \mu_{K,n}^\gamma(u)\big|\bigg).$$

Proof. By the definitions (2.11) and (4.1), we have for $\gamma \in \mathcal{E}_K$ and $n \in \mathcal{N}_\gamma$

$$\int_\gamma (\boldsymbol{\sigma}_h - \Pi_h^{RT}\boldsymbol{\sigma}) \cdot \boldsymbol{n}_K \, \theta_n^1 \, ds = \mu_{K,n}^\gamma - \mu_{K,n}^\gamma(u),$$
$$\int_K (\boldsymbol{\sigma}_h - \Pi_h^{RT}\boldsymbol{\sigma}) \, dx = \int_K a\nabla(u_h - u) \, dx.$$

The following inequality for $\boldsymbol{\tau}_h \in RT_1(K)$ can be obtained by the scaling argument

$$\|\boldsymbol{\tau}_h\|_{0,K} \le C\bigg(h_K^{-1} \bigg| \int_K \boldsymbol{\tau}_h \, dx \bigg| + \sum_{\gamma\in\mathcal{E}_K} \sum_{n\in\mathcal{N}_\gamma} \bigg| \int_\gamma \boldsymbol{\tau}_h \cdot \boldsymbol{n}_K \, \theta_n^1 \, ds \bigg| \bigg).$$

With $\boldsymbol{\tau}_h = \boldsymbol{\sigma}_h - \Pi_h^{RT}\boldsymbol{\sigma}$, it follows that

$$\|\boldsymbol{\sigma}_h - \Pi_h^{RT}\boldsymbol{\sigma}\|_{0,K} \le C\bigg(h_K^{-1} \bigg| \int_K a\nabla(u - u_h) \, dx \bigg| + \sum_{\gamma\in\mathcal{E}_K} \sum_{n\in\mathcal{N}_\gamma} \big| \mu_{K,n}^\gamma - \mu_{K,n}^\gamma(u) \big| \bigg). \quad (6.1)$$

To further bound the first term, let a_K be a constant such that $\|a - a_K\|_{0,\infty,K} \le Ch_K$ and observe that (2.7) gives

$$\int_K a_K \nabla(u - u_I) \, dx = \int_{\partial K} (u - u_I) a_K \boldsymbol{n}_K \, ds = 0.$$

By the Cauchy–Schwarz inequality and the interpolation error estimate (2.8), we obtain

$$\begin{aligned} h_K^{-1} \bigg| \int_K a\nabla(u - u_h) \, dx \bigg| &\le h_K^{-1} \bigg| \int_K (a - a_K)\nabla(u - u_I) \, dx \bigg| + h_K^{-1} \bigg| \int_K a\nabla(u_I - u_h) \, dx \bigg| \\ &\le C(\|a - a_K\|_{0,\infty,K} \|\nabla(u - u_I)\|_{0,K} + \|\nabla(u_I - u_h)\|_{0,K}) \\ &\le C(h_K^3 |u|_{3,K} + \|\nabla(u_I - u_h)\|_{0,K}). \end{aligned} \quad (6.2)$$

The proof is completed by combining (6.1)–(6.2). □

Now we need to estimate the flux moment error $\big|\mu_{K,n}^\gamma - \mu_{K,n}^\gamma(u)\big|$, and this will be done in each vertex patch. In Section 3 it was stated that for each vertex $n \in \mathcal{N}_h$, the vector $\boldsymbol{b}_n$ of equilibrated flux moments associated with n is the unique solution of the matrix system (3.6). It turns out that the corresponding vector $\boldsymbol{b}_n(u)$ of exact flux moments associated with vertex n is the solution of the same matrix system (3.7) with a similar right-hand side.

Lemma 6.2. *The vector $\boldsymbol{b}_n(u)$ is the solution of* (3.7) *with the right-hand side*

$$\boldsymbol{y} = \boldsymbol{y}_n(u), \qquad z = \boldsymbol{\nu}_N^T \boldsymbol{b}_n(u).$$

Proof. Since the last equation of (3.7) is obvious, it suffices to verify the equations corresponding to (3.3)–(3.5). First, we obtain for $1 \le i \le N$

$$\begin{aligned}\mu_{i,n}^{\gamma_i}(u) + \mu_{i,n}^{\gamma_{i+1}}(u) &= \int_{\gamma_i} a\nabla u \cdot \boldsymbol{n}_{K_i}\, \theta_n^1\, ds + \int_{\gamma_{i+1}} a\nabla u \cdot \boldsymbol{n}_{K_i}\, \theta_n^1\, ds \\ &= \int_{\partial K_i} a\nabla u \cdot \boldsymbol{n}_{K_i}\, \theta_n^1\, ds \\ &= \int_{K_i} a\nabla u \cdot \nabla\theta_n^1\, dx + \int_{K_i} \operatorname{div}(a\nabla u)\theta_n^1\, dx \\ &= \int_{K_i} a\nabla u \cdot \nabla\theta_n^1\, dx + \int_{K_i} cu\theta_n^1\, dx - \int_{K_i} f\theta_n^1\, dx \\ &= B_{K_i}(u, \theta_n^1) - (f, \theta_n^1)_{K_i} = \Delta_i(u), \end{aligned} \tag{6.3}$$

which exactly gives the first N equations of (3.7) corresponding to (3.3). The equations corresponding to (3.5) are

$$\mu_{i-1,n}^{\gamma_i}(u) + \mu_{i,n}^{\gamma_i}(u) = 0 \qquad (2 \le i \le N), \tag{6.4}$$

which hold true due to continuity of the exact normal fluxes. The remaining equation corresponding to (3.4) follows directly from (6.3)–(6.4). □

As a consequence of Lemma 6.2, we get the following result.

Lemma 6.3. *We have for all* $n \in \mathcal{N}_h$

$$\sum_{K\in\mathcal{T}_n} \sum_{\gamma\in\mathcal{E}_K\cap\mathcal{E}_n} \left|\mu_{K,n}^{\gamma} - \mu_{K,n}^{\gamma}(u)\right| \le C\Bigg(\sum_{K\in\mathcal{T}_n} \left|B_K(u-u_h, \theta_n^1)\right| + \left|\boldsymbol{\nu}_N^T \boldsymbol{b}_n(u-u_h)\right| \Bigg).$$

Proof. By the definitions of $\boldsymbol{b}_n$ and $\boldsymbol{b}_n(u)$, there exists a constant $C > 0$ such that

$$\sum_{K\in\mathcal{T}_n} \sum_{\gamma\in\mathcal{E}_K\cap\mathcal{E}_n} \left|\mu_{K,n}^{\gamma} - \mu_{K,n}^{\gamma}(u)\right| \le C|\boldsymbol{b}_n - \boldsymbol{b}_n(u)|.$$

It follows from Lemma 6.2 that the vector $\boldsymbol{x} = \boldsymbol{b}_n - \boldsymbol{b}_n(u)$ is the solution of (3.7) with the right-hand side

$$\boldsymbol{y} = \boldsymbol{y}_n(u_h) - \boldsymbol{y}_n(u) = \left[\, B_{K_i}(u_h - u, \theta_n^1) \,\right]_{i=1,2,\cdots,N}, \qquad z = \boldsymbol{\nu}_N^T \boldsymbol{b}_n(u_h - u),$$

and hence the stability result of Lemma 3.1 proves the assertion. □

The next thing to do is to estimate the right-hand side of the inequality given in Lemma 6.3. In what follows, we assign a unit normal $\boldsymbol{n}_\gamma$ to each edge $\gamma \in \mathcal{E}_n$ which is oriented clockwise around n, and set $\langle w\rangle|_\gamma = \frac{1}{2}(w|_K + w|_{K'})$ for each interior edge $\gamma = \partial K \cap \partial K'$.

Lemma 6.4. *We have for all* $n \in \mathcal{N}_h$

$$\sum_{K\in\mathcal{T}_n} \left|B_K(u-u_h, \theta_n^1)\right| + \left|\boldsymbol{\nu}_N^T \boldsymbol{b}_n(u-u_h)\right| \le C(h^3|u|_{3,\omega_n} + |\!|\!| u_I - u_h |\!|\!|_{\omega_n} + |I_n(a,u)|),$$

where the bilinear form $I_n(\cdot,\cdot)$ is defined by

$$I_n(a,u) := \sum_{\gamma\in\mathcal{E}_n\cap\mathcal{E}_\Omega}\int_\gamma \left(a\nabla u\cdot\boldsymbol{n}_\gamma - \langle a\nabla u_I\cdot\boldsymbol{n}_\gamma\rangle\right)\theta_n^1\,ds + \frac{1}{2}\sum_{\gamma\in\mathcal{E}_n\cap\mathcal{E}_{\partial\Omega}}\int_\gamma a\nabla(u-u_I)\cdot\boldsymbol{n}_\gamma\,\theta_n^1\,ds$$

Proof. Let a_K be a constant matrix such that $\|a-a_K\|_{0,\infty,K}\le Ch_K$. Since (2.7) gives

$$(a_K\nabla(u-u_I),\nabla\theta_n^1)_K = \int_{\partial K}(u-u_I)\,a_K\nabla\theta_n^1\cdot\boldsymbol{n}_K\,ds = 0,$$

it follows by the interpolation error estimate (2.8) and the estimate $|\!|\!|\theta_n^1|\!|\!|_K\le C$ that

$$\left|B_K(u-u_I,\theta_n^1)\right| = \left|((a-a_K)\nabla(u-u_I),\nabla\theta_n^1)_K + (c(u-u_I),\theta_n^1)_K\right| \le Ch_K^3|u|_{3,K},$$

and thus

$$\sum_{K\in\mathcal{T}_n}\left|B_K(u-u_h,\theta_n^1)\right| \le C(h^3|u|_{3,\omega_n} + |\!|\!|u_I-u_h|\!|\!|_{\omega_n}).$$

To estimate the remaining term, we observe that

$$\begin{aligned}\boldsymbol{\nu}_N^T\boldsymbol{b}_n(w) &= \sum_{i=1}^N\left(\int_{\gamma_i}a\nabla w|_{K_i}\cdot\boldsymbol{n}_{K_i}\,\theta_n^1\,ds - \int_{\gamma_{i+1}}a\nabla w|_{K_i}\cdot\boldsymbol{n}_{K_i}\,\theta_n^1\,ds\right)\\ &= -2\sum_{\gamma\in\mathcal{E}_n\cap\mathcal{E}_\Omega}\int_\gamma\langle a\nabla w\cdot\boldsymbol{n}_\gamma\rangle\,\theta_n^1\,ds - \sum_{\gamma\in\mathcal{E}_n\cap\mathcal{E}_{\partial\Omega}}\int_\gamma a\nabla w\cdot\boldsymbol{n}_\gamma\,\theta_n^1\,ds.\end{aligned}$$

From this result it follows that

$$\left|\boldsymbol{\nu}_N^T\boldsymbol{b}_n(u-u_I)\right| = 2|I_n(a,u)|,$$

$$\left|\boldsymbol{\nu}_N^T\boldsymbol{b}_n(u_I-u_h)\right| \le C\sum_{K\in\mathcal{T}_n}\|\nabla(u_I-u_h)\|_{0,\partial K}\|\theta_n^1\|_{0,\partial K} \le C\|\nabla(u_I-u_h)\|_{0,\omega_n},$$

where we used the local inverse inequality $\|v\|_{0,\partial K}\le Ch_K^{-1/2}\|v\|_{0,K}$ for a polynomial v and the estimate $\|\theta_n^1\|_{0,K}\le Ch_K$. Hence we obtain

$$\left|\boldsymbol{\nu}_N^T\boldsymbol{b}_n(u-u_h)\right| \le C(|I_n(a,u)| + \|\nabla(u_I-u_h)\|_{0,\omega_n}),$$

which completes the proof. □

Now we are in a position to prove Theorem 4.1.

Proof of Theorem 4.1. Since the number of elements in $\mathcal{T}_n$ is uniformly bounded for all $n\in\mathcal{N}_h$, it follows from Lemmas 6.1, 6.3 and 6.4 that

$$\|\boldsymbol{\sigma}_h - \Pi_h^{RT}\boldsymbol{\sigma}\|_{0,\Omega} \le C\left\{h^3|u|_{3,\Omega} + |\!|\!|u_I-u_h|\!|\!|_\Omega + \left(\sum_{n\in\mathcal{N}_h}|I_n(a,u)|^2\right)^{1/2}\right\}. \tag{6.5}$$

The error estimates (2.4) and (2.8) immediately give

$$|\!|\!| u_I - u_h |\!|\!|_\Omega \le |\!|\!| u - u_I |\!|\!|_\Omega + |\!|\!| u - u_h |\!|\!|_\Omega \le Ch^2 \|u\|_{3,\Omega}.$$

Using the local trace inequality

$$\int_{\partial K} |f|\, ds \le C\left(h_K^{-1} \int_K |f|\, dx + \int_K |\nabla f|\, dx \right) \le C(\|f\|_{0,K} + h_K |f|_{1,K})$$

and the interpolation error estimate (2.8), we obtain for all $n \in \mathcal{N}_h$

$$\begin{aligned} |I_n(a,u)| &\le C \sum_{K \in \mathcal{T}_n} \int_{\partial K} \left| a \nabla (u - u_I) \cdot \boldsymbol{n}_K \right| ds \\ &\le C \sum_{K \in \mathcal{T}_n} \left(|u - u_I|_{1,K} + h_K |u - u_I|_{2,K} \right) \le Ch^2 |u|_{3,\omega_n}. \end{aligned} \tag{6.6}$$

Collecting the above results yields

$$\|\boldsymbol{\sigma}_h - \Pi_h^{RT} \boldsymbol{\sigma}\|_{0,\Omega} \le Ch^2 \|u\|_{3,\Omega},$$

and thus it follows by (2.13) that

$$\|\boldsymbol{\sigma} - \boldsymbol{\sigma}_h\|_{0,\Omega} \le \|\boldsymbol{\sigma} - \Pi_h^{RT} \boldsymbol{\sigma}\|_{0,\Omega} + \|\boldsymbol{\sigma}_h - \Pi_h^{RT} \boldsymbol{\sigma}\|_{0,\Omega} \le Ch^2 \|u\|_{3,\Omega}.$$

This completes the proof of Theorem 4.1. □

To prove Theorem 4.2, we need to improve the estimate (6.6) in the subregion where the triangulation is nearly uniform. This is done in the following lemma whose proof is rather long.

Lemma 6.5. *Let $\mathcal{N}_{1,h} = \{n \in \mathcal{N}_\Omega : \mathcal{T}_n \subset \mathcal{T}_{1,h}\}$. Then we have for all $n \in \mathcal{N}_{1,h}$*

$$|I_n(a,u)| \le Ch^{2+\min(\alpha,1)} \|u\|_{4,\omega_n}$$

if the mesh size h is sufficiently small.

Proof. Let a_{ω_n} be a constant matrix and let w be a cubic polynomial over ω_n such that $\|a - a_{\omega_n}\|_{0,\infty,\omega_n} \le Ch$ and $|u - w|_{3,\omega_n} \le Ch \|u\|_{4,\omega_n}$ (see [31] for construction of such a polynomial). Then, by the same argument leading to (6.6), we obtain

$$\begin{aligned} |I_n(a - a_{\omega_n}, u)| &\le C \|a - a_{\omega_n}\|_{0,\infty,\omega_n} \cdot h^2 |u|_{3,\omega_n} \le Ch^3 |u|_{3,\omega_n}, \\ |I_n(a_{\omega_n}, u - w)| &\le Ch^2 |u - w|_{3,\omega_n} \le Ch^3 \|u\|_{4,\omega_n}, \end{aligned}$$

and hence

$$\begin{aligned} |I_n(a,u)| &= |I_n(a - a_{\omega_n}, u) + I_n(a_{\omega_n}, u - w) + I_n(a_{\omega_n}, w)| \\ &\le Ch^3 \|u\|_{4,\omega_n} + |I_n(a_{\omega_n}, w)|. \end{aligned}$$

Since $|w|_{3,\omega_n} \le |w - u|_{3,\omega_n} + |u|_{3,\omega_n} \le C\|u\|_{4,\omega_n}$, the assertion is proved if we show that

$$|I_n(a_{\omega_n}, w)| \le Ch^{2+\alpha} |w|_{3,\omega_n}. \tag{6.7}$$

The proof of (6.7) is divided into two parts (note that $\mathcal{E}_n \subset \mathcal{E}_\Omega$ for $n \in \mathcal{N}_{1,h}$)

$$\left| \sum_{\gamma\in\mathcal{E}_n} \int_\gamma \big(a_{\omega_n}\nabla w\cdot \boldsymbol{n}_\gamma - \langle a_{\omega_n}\nabla w_I\cdot\boldsymbol{n}_\gamma\rangle\big)(\theta_n^1 - \tfrac{1}{2})\,ds\right| \le Ch^{2+\alpha}|w|_{3,\omega_n}, \tag{6.8}$$

$$\left| \sum_{\gamma\in\mathcal{E}_n} \int_\gamma \big(a_{\omega_n}\nabla w\cdot \boldsymbol{n}_\gamma - \langle a_{\omega_n}\nabla w_I\cdot\boldsymbol{n}_\gamma\rangle\big)\,ds\right| \le Ch^{2+\alpha}|w|_{3,\omega_n}. \tag{6.9}$$

Let us first prove (6.8) by showing that for all $\gamma \in \mathcal{E}_n$,

$$\left| \int_\gamma (\nabla w - \langle\nabla w_I\rangle)(\theta_n^1 - \tfrac{1}{2})\,ds\right| \le Ch^{2+\alpha}|w|_{3,\omega_n}. \tag{6.10}$$

As in the proof of [3, Lemma 4.1], we use the following Taylor expansions

$$\nabla w|_\gamma = \nabla w(m_\gamma) + s\frac{\partial}{\partial \boldsymbol{t}_\gamma}(\nabla w)(m_\gamma) + \frac{s^2}{2}\frac{\partial^2}{\partial \boldsymbol{t}_\gamma^2}(\nabla w),$$
$$\langle\nabla w_I\rangle|_\gamma = \langle\nabla w_I\rangle(m_\gamma) + s\frac{\partial}{\partial \boldsymbol{t}_\gamma}\langle\nabla w_I\rangle,$$

where $s \in [-l_\gamma/2, l_\gamma/2]$ is a parameter for γ with the length l_γ and the midpoint m_γ, and $\boldsymbol{t}_\gamma$ is the unit tangent obtained from $\boldsymbol{n}_\gamma$ by 90° counterclockwise rotation. Substitution of these expressions and $\theta_n^1 - 1/2|_\gamma = s/l_\gamma$ into (6.10) gives

$$\int_\gamma (\nabla w - \langle\nabla w_I\rangle)(\theta_n^1 - \tfrac{1}{2})\,ds = \left(\frac{\partial}{\partial \boldsymbol{t}_\gamma}(\nabla w)(m_\gamma) - \frac{\partial}{\partial \boldsymbol{t}_\gamma}\langle\nabla w_I\rangle\right)\int_{-l_\gamma/2}^{l_\gamma/2}\frac{s^2}{l_\gamma}\,ds. \tag{6.11}$$

Since $\mathcal{T}_n \subset \mathcal{T}_{1,h}$, we deduce from [3, Lemma 3.1–3.2] that

$$\frac{\partial}{\partial \boldsymbol{t}_\gamma}(\nabla w\cdot\boldsymbol{t}_\gamma)(m_\gamma) - \frac{\partial}{\partial \boldsymbol{t}_\gamma}\langle\nabla w_I\cdot\boldsymbol{t}_\gamma\rangle = \frac{\partial^2 w}{\partial \boldsymbol{t}_\gamma^2}(m_\gamma) - \frac{\partial^2 w_I}{\partial \boldsymbol{t}_\gamma^2} = 0,$$
$$\left|\frac{\partial}{\partial \boldsymbol{t}_\gamma}(\nabla w\cdot\boldsymbol{n}_\gamma)(m_\gamma) - \frac{\partial}{\partial \boldsymbol{t}_\gamma}\langle\nabla w_I\cdot\boldsymbol{n}_\gamma\rangle\right| \le Ch^{1+\alpha}|w|_{3,\infty,\omega_n}.$$

By the local inverse inequality $|w|_{3,\infty,K} \le Ch_K^{-1}|w|_{3,K}$ for $K \in \mathcal{T}_n$, it follows that

$$\left|\frac{\partial}{\partial \boldsymbol{t}_\gamma}(\nabla w)(m_\gamma) - \frac{\partial}{\partial \boldsymbol{t}_\gamma}\langle\nabla w_I\rangle\right| \le Ch^{\alpha}|w|_{3,\omega_n},$$

and (6.10) is immediately obtained from this result and (6.11).

To prove the second part (6.9), we use the fact that for sufficiently small mesh size, $\mathcal{T}_n$ contains six triangles $K_1, K_2, K_3, K_1', K_2', K_3'$ (clockwise arranged) such that K_i is $O(h^{1+\alpha})$-perturbation of K_i' for $1 \le i \le 3$ (see [4, Lemma 8.1] and its proof). Since every edge of $\mathcal{E}_n$ is

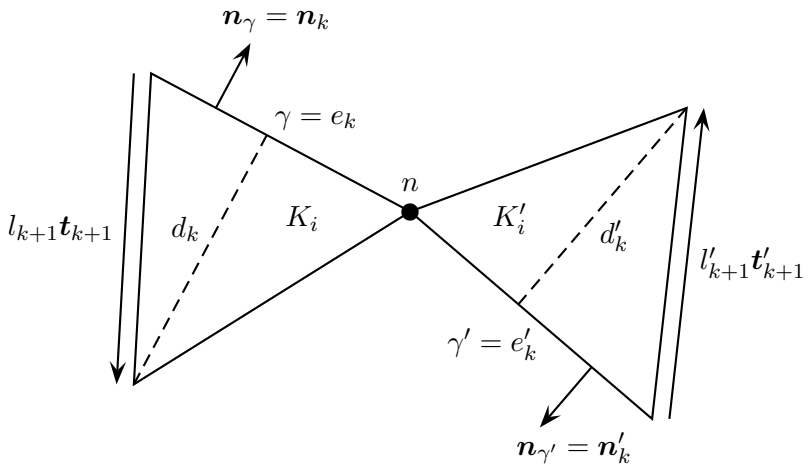

FIGURE 3. Notation for the triangle K_i and the corresponding triangle K_i'.

shared by two triangles, it is easy to see that

$$\sum_{\gamma\in\mathcal{E}_n}\int_\gamma \left(a_{\omega_n}\nabla w\cdot\boldsymbol{n}_\gamma - \langle a_{\omega_n}\nabla w_I\cdot\boldsymbol{n}_\gamma\rangle\right) ds$$
$$= \frac{1}{2}\sum_{1\le i\le 3}\Bigg\{\sum_{\gamma\in\mathcal{E}_n\cap\mathcal{E}_{K_i}}\int_\gamma a_{\omega_n}\nabla(w-w_I)|_{K_i}\cdot\boldsymbol{n}_\gamma\, ds + \sum_{\gamma'\in\mathcal{E}_n\cap\mathcal{E}_{K_i'}}\int_{\gamma'} a_{\omega_n}\nabla(w-w_I)|_{K_i'}\cdot\boldsymbol{n}_{\gamma'}\, ds\Bigg\}.$$

Then the result (6.9) follows by showing that

$$\left|\int_\gamma a_{\omega_n}\nabla(w-w_I)|_{K_i}\cdot\boldsymbol{n}_\gamma\, ds + \int_{\gamma'} a_{\omega_n}\nabla(w-w_I)|_{K_i'}\cdot\boldsymbol{n}_{\gamma'}\, ds\right| \le Ch^{2+\alpha}|w|_{3,\omega_n} \quad (6.12)$$

for every pair of corresponding edges $\gamma\in\mathcal{E}_{K_i}$ and $\gamma'\in\mathcal{E}_{K_i'}$ as depicted in Fig. 3.

To use some results from [28], we borrow additional notation from [28, Section 2]. Let e_k be an edge of K_i opposite to the k-th vertex of K_i for $1\le k\le 3$. We denote the length, the perpendicular height, the unit outward normal and counterclockwise tangent vectors of e_k by l_k, d_k, $\boldsymbol{n}_k$ and $\boldsymbol{t}_k$, respectively, and mark the corresponding quantities on K_i' by primes; see Fig. 3 for an illustration. By convention the subscripts are understood to be cyclic modulo 3.

Let $\{\phi_k\}_{k=1}^3$ be the barycentric coordinates on K_i and define the cubic polynomials $\psi_0 = \phi_1\phi_2\phi_3$ and $\psi_k = \phi_{k+1}^2\phi_{k+2} - \phi_{k+1}\phi_{k+2}^2$ for $1\le k\le 3$ which satisfy

$$\psi_0|_{\partial K_i} = 0, \qquad \psi_k|_{\partial K_i\setminus e_k} = 0, \qquad \int_{e_k}\psi_k\, ds = 0.$$

Then we have

$$\nabla\phi_k = -\frac{\boldsymbol{n}_k}{d_k}, \quad \psi_k = \frac{l_k}{2}\frac{\partial}{\partial \boldsymbol{t}_k}(\phi_{k+1}^2\phi_{k+2}^2), \quad \int_{e_k}\nabla(\phi_k^2)\,ds = \int_{e_k} 2\phi_k\nabla\phi_k\,ds = 0,$$

and a direct calculation shows that

$$\int_{e_k}\nabla\psi_0\,ds = \nabla\phi_k\int_{e_k}\phi_{k+1}\phi_{k+2}\,ds = -\frac{l_k}{6d_k}\boldsymbol{n}_k,$$

$$\int_{e_k}\nabla\psi_k\,ds = l_k\int_{e_k}\frac{\partial}{\partial \boldsymbol{t}_k}\big\{\phi_{k+1}\phi_{k+2}\nabla(\phi_{k+1}\phi_{k+2})\big\}\,ds = 0,$$

$$\int_{e_k}\nabla\psi_{k+1}\,ds = \nabla\phi_k\int_{e_k}\phi_{k+2}^2\,ds = -\frac{l_k}{3d_k}\boldsymbol{n}_k,$$

$$\int_{e_k}\nabla\psi_{k+2}\,ds = -\nabla\phi_k\int_{e_k}\phi_{k+1}^2\,ds = \frac{l_k}{3d_k}\boldsymbol{n}_k.$$

Combining these results with the following equality from [28, Lemma 2.3]

$$w - w_I = \bigg(\sum_{j=1}^{3}\frac{l_j^2 l_{j+1}}{6}\frac{\partial^3 w}{\partial \boldsymbol{t}_j^2\partial \boldsymbol{t}_{j+1}} + \frac{l_1 l_2 l_3}{4}\frac{\partial^3 w}{\partial \boldsymbol{t}_1\partial \boldsymbol{t}_2\partial \boldsymbol{t}_3}\bigg)\psi_0 + \sum_{j=1}^{3}\frac{l_j^3}{12}\frac{\partial^3 w}{\partial \boldsymbol{t}_j^3}\,\psi_j,$$

we obtain for $\gamma = e_k$

$$\int_\gamma a_{\omega_n}\nabla(w - w_I)|_{K_i}\cdot\boldsymbol{n}_\gamma\,ds = \bigg\{-\sum_{j=1}^{3}\frac{l_j^2 l_{j+1}}{36}\frac{\partial^3 w}{\partial \boldsymbol{t}_j^2\partial \boldsymbol{t}_{j+1}} - \frac{l_1 l_2 l_3}{24}\frac{\partial^3 w}{\partial \boldsymbol{t}_1\partial \boldsymbol{t}_2\partial \boldsymbol{t}_3} - \frac{l_{k+1}^3}{36}\frac{\partial^3 w}{\partial \boldsymbol{t}_{k+1}^3} + \frac{l_{k+2}^3}{36}\frac{\partial^3 w}{\partial \boldsymbol{t}_{k+2}^3}\bigg\}\frac{l_k}{d_k}\boldsymbol{n}_k\cdot a_{\omega_n}\boldsymbol{n}_k, \quad (6.13)$$

and similarly

$$\int_{\gamma'} a_{\omega_n}\nabla(w - w_I)|_{K_i'}\cdot\boldsymbol{n}_{\gamma'}\,ds = \bigg\{-\sum_{j=1}^{3}\frac{{l_j'}^2 l_{j+1}'}{36}\frac{\partial^3 w}{\partial {\boldsymbol{t}_j'}^2\partial \boldsymbol{t}_{j+1}'} - \frac{l_1' l_2' l_3'}{24}\frac{\partial^3 w}{\partial \boldsymbol{t}_1'\partial \boldsymbol{t}_2'\partial \boldsymbol{t}_3'} - \frac{{l'}_{k+1}^3}{36}\frac{\partial^3 w}{\partial {\boldsymbol{t}'}_{k+1}^3} + \frac{{l'}_{k+2}^3}{36}\frac{\partial^3 w}{\partial {\boldsymbol{t}'}_{k+2}^3}\bigg\}\frac{l_k'}{d_k'}\boldsymbol{n}_k'\cdot a_{\omega_n}\boldsymbol{n}_k'. \quad (6.14)$$

Now we prove (6.12) by the usual argument of using the telescoping type inequality given in [32]. Note that the third derivatives of w are constant over ω_n and

$$l_i l_j l_k\frac{\partial^3 w}{\partial \boldsymbol{t}_i\partial \boldsymbol{t}_j\partial \boldsymbol{t}_k} = \sum_{1\le p,q,r\le 2} l_i l_j l_k t_i^p t_j^q t_k^r\frac{\partial^3 w}{\partial x_p\partial x_q\partial x_r},$$

$$l_i' l_j' l_k'\frac{\partial^3 w}{\partial \boldsymbol{t}_i'\partial \boldsymbol{t}_j'\partial \boldsymbol{t}_k'} = \sum_{1\le p,q,r\le 2} l_i' l_j' l_k' {t_i'}^p {t_j'}^q {t_k'}^r\frac{\partial^3 w}{\partial x_p\partial x_q\partial x_r},$$

where $\boldsymbol{t}_i = (t_i^1, t_i^2)$ and $\boldsymbol{t}_i' = (t_i'^1, t_i'^2)$. Since K_i is $O(h^{1+\alpha})$-perturbation of K_i', we have

$$|l_i - l_i'| + |d_i - d_i'| \le Ch^{1+\alpha}, \qquad |\boldsymbol{t}_i + \boldsymbol{t}_i'| + |\boldsymbol{n}_i + \boldsymbol{n}_i'| \le Ch^{\alpha}.$$

Hence it follows from (6.13)–(6.14) that

$$\left| \int_{\gamma} a_{\omega_n} \nabla (w - w_I)|_{K_i} \cdot \boldsymbol{n}_{\gamma}\, ds + \int_{\gamma'} a_{\omega_n} \nabla (w - w_I)|_{K_i'} \cdot \boldsymbol{n}_{\gamma'}\, ds \right| \le Ch^{3+\alpha} |w|_{3,\infty,\omega_n},$$

which gives (6.12) by the local inverse inequality $|w|_{3,\infty,K} \le Ch_K^{-1}|w|_{3,K}$ for $K \in \mathcal{T}_n$. □

Now we are ready to prove Theorem 4.2.

Proof of Theorem 4.2. We need to estimate the third term in (6.5). Since the number of elements in $\mathcal{T}_n$ is uniformly bounded for all $n \in \mathcal{N}_h$, it follows from Lemma 6.5 that

$$\Big(\sum_{n \in \mathcal{N}_{1,h}} |I_n(a,u)|^2 \Big)^{1/2} \le Ch^{2+\min(\alpha,1)} \|u\|_{4,\Omega}.$$

On the other hand, we obtain by Condition (α, σ)

$$\sum_{n \in \mathcal{N}_h \setminus \mathcal{N}_{1,h}} |\omega_n| = \sum_{n \in \mathcal{N}_\Omega \setminus \mathcal{N}_{1,h}} |\omega_n| + \sum_{n \in \mathcal{N}_{\partial\Omega}} |\omega_n| \le Ch^{\sigma} + Ch \le Ch^{\min(\sigma,1)},$$

and thus by (6.6)

$$\begin{aligned} \Big(\sum_{n \in \mathcal{N}_h \setminus \mathcal{N}_{1,h}} |I_n(a,u)|^2 \Big)^{1/2} &\le Ch^2 \Big(\sum_{n \in \mathcal{N}_h \setminus \mathcal{N}_{1,h}} |u|_{3,\omega_n}^2 \Big)^{1/2} \\ &\le Ch^2 \Big(\sum_{n \in \mathcal{N}_h \setminus \mathcal{N}_{1,h}} |\omega_n| \Big)^{1/2} |u|_{3,\infty,\Omega} \\ &\le Ch^{2+\min(\frac{\sigma}{2},\frac{1}{2})} |u|_{3,\infty,\Omega}. \end{aligned}$$

Collecting the two results above yields

$$\Big(\sum_{n \in \mathcal{N}_h} |I_n(a,u)|^2 \Big)^{1/2} \le Ch^{2+\min(\alpha,\frac{\sigma}{2},\frac{1}{2})} (\|u\|_{4,\Omega} + |u|_{3,\infty,\Omega}).$$

The proof of Theorem 4.2 is completed by applying this result and (2.9) in (6.5). □

REFERENCES

[1] R. E. Bank and A. Weiser, *Some a posteriori error estimators for elliptic partial differential equations*, Math. Comp., **44** (1985), 283–301.

[2] R. G. Durán and R. Rodríguez, *On the asymptotic exactness of Bank–Weiser's estimator*, Numer. Math., **62** (1992), 297–303.

[3] K.-Y. Kim and J.-S. Park, *Asymptotic exactness of some Bank–Weiser error estimator for quadratic triangular finite element*, Bull. Korean Math. Soc., **57** (2020), 393–406.

[4] A. Maxim, *Asymptotic exactness of an a posteriori error estimator based on the equilibrated residual method*, Numer. Math., **106** (2007), 225–253.
[5] R. E. Bank and J. Xu, *Asymptotically exact a posteriori error estimators, part I: grids with superconvergence*, SIAM J. Numer. Anal., **41** (2003), 2294–2312.
[6] N. Levine, *Superconvergent recovery of the gradient from piecewise linear finite-element approximations*, IMA J. Numer. Anal., **5** (1985), 407–427.
[7] A. Naga and Z. Zhang, *A posteriori error estimates based on the polynomial preserving recovery*, SIAM J. Numer. Anal., **42** (2004), 1780–1800.
[8] J. Xu and Z. Zhang, *Analysis of recovery type a posteriori error estimators for mildly structured grids*, Math. Comp., **73** (2004), 1139–1152.
[9] O. C. Zienkiewicz and J. Z. Zhu, *The superconvergent patch recovery (SPR) and adaptive finite element refinement*, Comput. Methods Appl. Mech. Engrg., **101** (1992), 207–224.
[10] W. Prager and J. L. Synge, *Approximations in elasticity based on the concept of function space*, Quart. Appl. Math., **5** (1947), 241–269.
[11] M. Ainsworth, *A framework for obtaining guaranteed error bounds for finite element approximations*, J. Comput. Appl. Math., **234** (2010), 2618–2632.
[12] D. Braess, V. Pillwein and J. Schöberl, *Equilibrated residual error estimates are p-robust*, Comput. Methods Appl. Mech. Engrg., **198** (2009), 1189–1197.
[13] D. Braess and J. Schöberl, *Equilibrated residual error estimator for edge elements*, Math. Comp., **77** (2008), 651–672.
[14] Z. Cai and S. Zhang, *Robust equilibrated residual error estimator for diffusion problems: conforming elements*, SIAM J. Numer. Anal., **50** (2012), 151–170.
[15] C. Carstensen and C. Merdon, *Effective postprocessing for equilibration a posteriori error estimators*, Numer. Math., **123** (2013), 425–459.
[16] P. Destuynder and B. Métivet, *Explicit error bounds in a conforming finite element method*, Math. Comp., **68** (1999), 1379–1396.
[17] A. Ern and M. Vohralík, *Polynomial-degree-robust a posteriori estimates in a unified setting for conforming, nonconforming, discontinuous Galerkin, and mixed discretizations*, SIAM J. Numer. Anal., **53** (2015), 1058–1081.
[18] R. Luce and B. I. Wohlmuth, *A local a posteriori error estimator based on equilibrated fluxes*, SIAM J. Numer. Anal., **42** (2004), 1394–1414.
[19] T. Vejchodský, *Guaranteed and locally computable a posteriori error estimate*, IMA J. Numer. Anal., **26** (2006), 525–540.
[20] R. Verfürth, *A note on constant-free a posteriori error estimates*, SIAM J. Numer. Anal., **47** (2009), 3180–3194.
[21] M. Vohralík, *Guaranteed and fully robust a posteriori error estimates for conforming discretizations of diffusion problems with discontinuous coefficients*, J. Sci. Comput., **46** (2011), 397–438.
[22] A. Ern and M. Vohralík, *Adaptive inexact Newton methods with a posteriori stopping criteria for nonlinear diffusion PDEs*, SIAM J. Sci. Comput., **35** (2013), A1761–A1791.
[23] P. Jiránek, Z. Strakoš and M. Vohralík, *A posteriori error estimates including algebraic error and stopping criteria for iterative solvers*, SIAM J. Sci. Comput., **32** (2010), 1567–1590.
[24] M. Ainsworth and J. T. Oden, *A posteriori error estimation in finite element analysis*, John Wiley & Sons, New York, 2000.
[25] K.-Y. Kim, *Postprocessing for guaranteed error bound based on equilibrated fluxes*, J. Korean Math. Soc., **52** (2015), 891–906.
[26] P. Grisvard, *Elliptic problems in non-smooth domains*, Monographs and studies in mathematics 24, Pitman, Boston, 1985.
[27] Q. Lin, H. Xie and J. Xu, *Lower bounds of the discretization error for piecewise polynomials*, Math. Comp., **83** (2014), 1–13.

[28] Y. Huang and J. Xu, *Superconvergence of quadratic finite elements on mildly structured grids*, Math. Comp., **77** (2008), 1253–1268.
[29] H. Wu and Z. Zhang, *Can we have superconvergent gradient recovery under adaptive meshes?*, SIAM J. Numer. Anal., **45** (2007), 1701–1722.
[30] D. Boffi, F. Brezzi and M. Fortin, *Mixed finite element methods and applications*, Springer series in computational mathematics 44, Springer, Heidelberg, 2013.
[31] S. C. Brenner and L. R. Scott, *The mathematical theory of finite element methods*, Springer, New York, 2008.
[32] R. E. Bank and Y. Li, *Superconvergent recovery of Raviart–Thomas mixed finite element on triangular grids*, J. Sci. Comput., **81** (2019), 1882–1905.